Supporting information

Giant Magnetoresistance and Tunneling Electroresistance in Multiferroic Tunnel Junctions with 2D Ferroelectrics

Yancong Chen,[1,2,3] Zhiyuan Tang, [1,2,3] Minzhi Dai, [1,2,3] Xin Luo, [1,2,3*] and Yue Zheng[1,2,3*]

[1] Guangdong Provincial Key Laboratory of Magnetoelectric Physics and Devices, School of Physics, Sun Yat-sen University, Guangzhou 510275, China

[2] State Key Laboratory of Optoelectronic Materials and Technologies, School of Physics, Sun Yat-sen University, Guangzhou 510275, China

[3] Centre for Physical Mechanics and Biophysics, School of Physics, Sun Yat-sen University, Guangzhou 510275, China

[*]**Email:** luox77@mail.sysu.edu.cn and zhengy35@mail.sysu.edu.cn

In our tunneling junction, the devices are divided into the left, right electrodes and central region. The tunneling probability is quantified by the transmission coefficient, which is obtained from the non-equilibrium Green's function method[1]:

$$t(\varepsilon) = G(\varepsilon)\Gamma^{L}(\varepsilon)G^{\dagger}(\varepsilon)\Gamma^{R}(\varepsilon), \tag{1}$$

where G is the retarded Green's function and Γ is the broadening function of the electrode, $\Gamma = \frac{1}{i}(\Sigma - \Sigma^{\dagger})$, given in terms of the electrode self energy Σ. The G matrix is obtained by inverting the Hamiltonian matrix of the central region:

$$G(\varepsilon) = \left[(\varepsilon + i\delta_{+})S - H - \Sigma^{L}(\varepsilon) - \Sigma^{R}(\varepsilon)\right]^{-1}, \tag{2}$$

where S and H is the overlap and Hamiltonian matrices, respectively, of the central region. δ_{+} is an infinitesimal positive number. $\Sigma^{L}(\varepsilon)$ and $\Sigma^{R}(\varepsilon)$ are respectively the self-energies of the left and right electrodes, which can be calculated from the electrode Hamiltonian.

The effective potential is the sum of the pseudopotential V_{ps}, the exchange-correlation potential V_{xc} and electrostatic Hartree potentials V_H. For V_{xc}, we used the GGA-PBE, and the projector augmented wave method is used for V_{ps}. In the zero bias, the calculation of the electrostatic Hartree potential V_H requires the consideration of the system as it could be obtained from the solution of the Poisson's equation, $\nabla V_H(r) = -4\pi n(r)$, using a fast Fourier transform technique. The Hartree potential $V_H(r)$ is determined from the electron charge density in the tunnel junction, which is decided by the materials and the interaction between them. The interaction in NIN and NIBN tunnel junction is mainly dominated by the polarization direction of In_2Se_3 layers and the interlayer distance. The interlayer distance in our model is optimized using the DFT-D3 method, which provides the correct interlayer spacing by considering the van-der-Waals interaction with dispersion force correction.

The transmission coefficient comes from the trace of the transmission matrix:

$$T(E) = \sum_{k_{\parallel}} \left| t_{\sigma}(E, k_{\parallel}) \right|^2 , \quad (3)$$

where $t_{\sigma}(E)$ is the transmission function from Bloch state in the left electrode to Bloch state in the right electrode with the transverse Bloch wave vector $k_{\parallel}$ at energy level E for spin σ. The spin-resolved conductance at zero bias is given by the Landauer-Büttiker formula:

$$G_{\sigma}(E) = \frac{e^2}{h} \sum_{k_{\parallel}} \left| t_{\sigma}(E, k_{\parallel}) \right|^2 = \frac{e^2}{h} T(E) . \quad (4)$$

The TMR ratio is obtained from:

$$TMR = \frac{G_p - G_{AP}}{G_{AP}} = \frac{T_p - T_{AP}}{T_{AP}} , \quad (5)$$

where G_p and G_{AP} are the conductance of device with $M_{\uparrow\uparrow}$ and $M_{\uparrow\downarrow}$ configurations, respectively. T_p and T_{AP} are the transmission coefficients of device with $M_{\uparrow\uparrow}$ and $M_{\uparrow\downarrow}$ configurations, respectively.

The TER ratio is calculated from:

$$TER = \frac{G_m - G_n}{\min\{G_m, G_n\}} = \frac{T_m - T_n}{\min\{T_m, T_n\}} , \quad (6)$$

where G_m and G_n are the conductance for different polarization states of MFTJ, and $m \neq n$. T_m and T_n are the transmission coefficients for different polarization states of MFTJ.

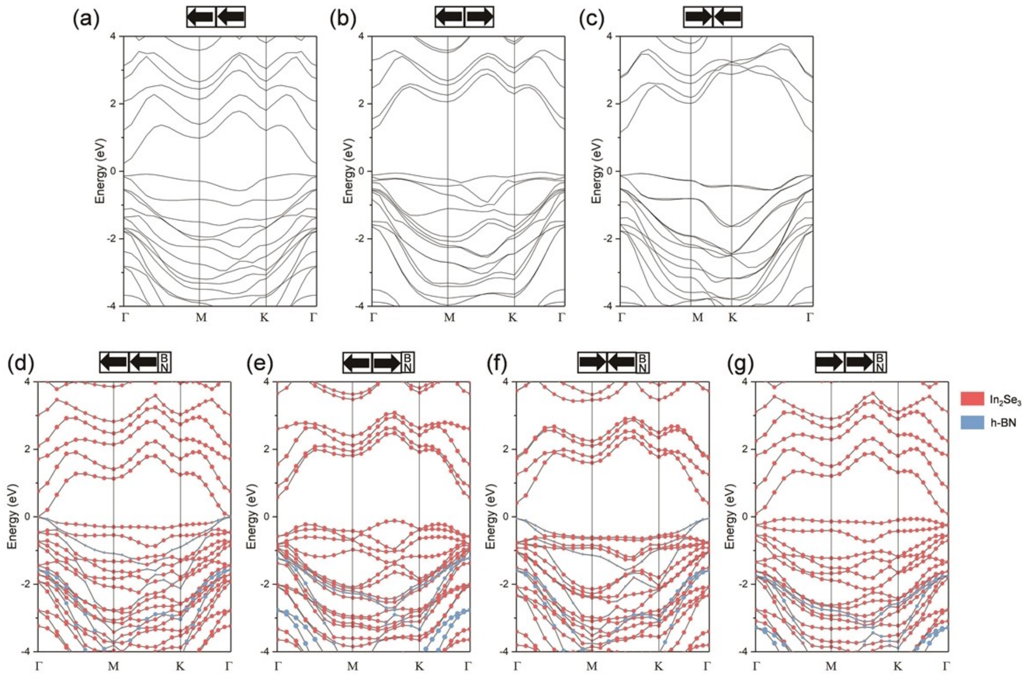

Fig. S1 HSE calculated band structures of (a)-(c) 2L-In_2Se_3 and (d)-(g) 2L-In_2Se_3/BN heterostructures.

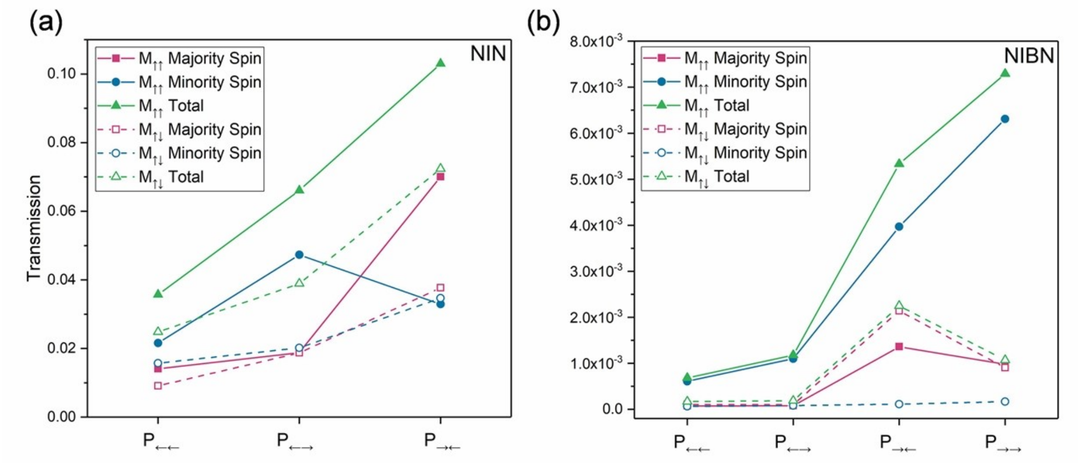

Fig. S2 Transmission coefficients of (a) NIN and (b) NIBN tunnel junctions in different magnetic polarization states.

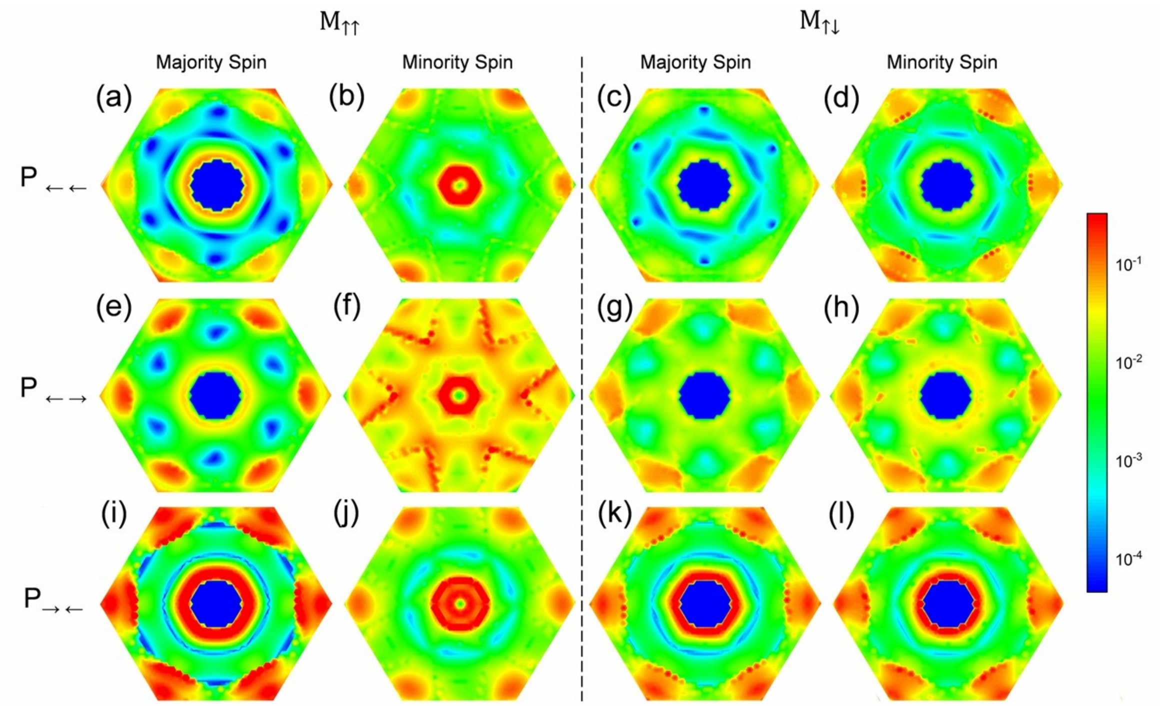

Fig. S3 k-resolved transmission spectrums for majority spin and minority spin conduction channels of NIN with (a)-(d) $P_{\leftarrow\leftarrow}$ barrier, (e)-(f) $P_{\leftarrow\rightarrow}$ barrier, and (i)-(l) $P_{\rightarrow\leftarrow}$ barrier under parallel ($M_{\uparrow\uparrow}$) and antiparallel ($M_{\uparrow\downarrow}$) magnetization of Ni electrodes.

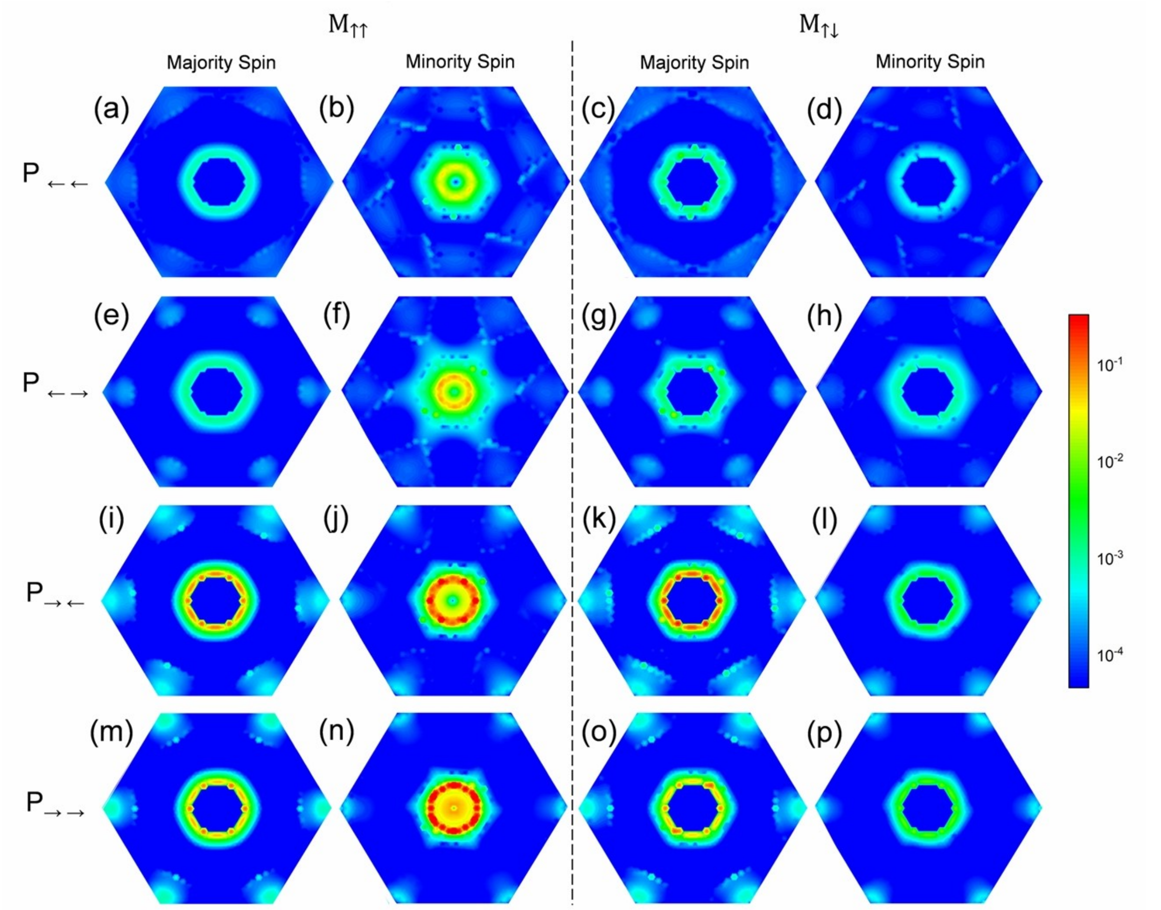

Fig. S4 k-resolved transmission spectrums for majority spin and minority spin conduction channels of NIBN with (a)-(d) $P_{\leftarrow\leftarrow}$ barrier, (e)-(f) $P_{\leftarrow\rightarrow}$ barrier, (i)-(l) $P_{\rightarrow\leftarrow}$ barrier, and (m)-(p) $P_{\rightarrow\rightarrow}$ barrier under parallel ($M_{\uparrow\uparrow}$) and antiparallel ($M_{\uparrow\downarrow}$) magnetization of Ni electrodes.

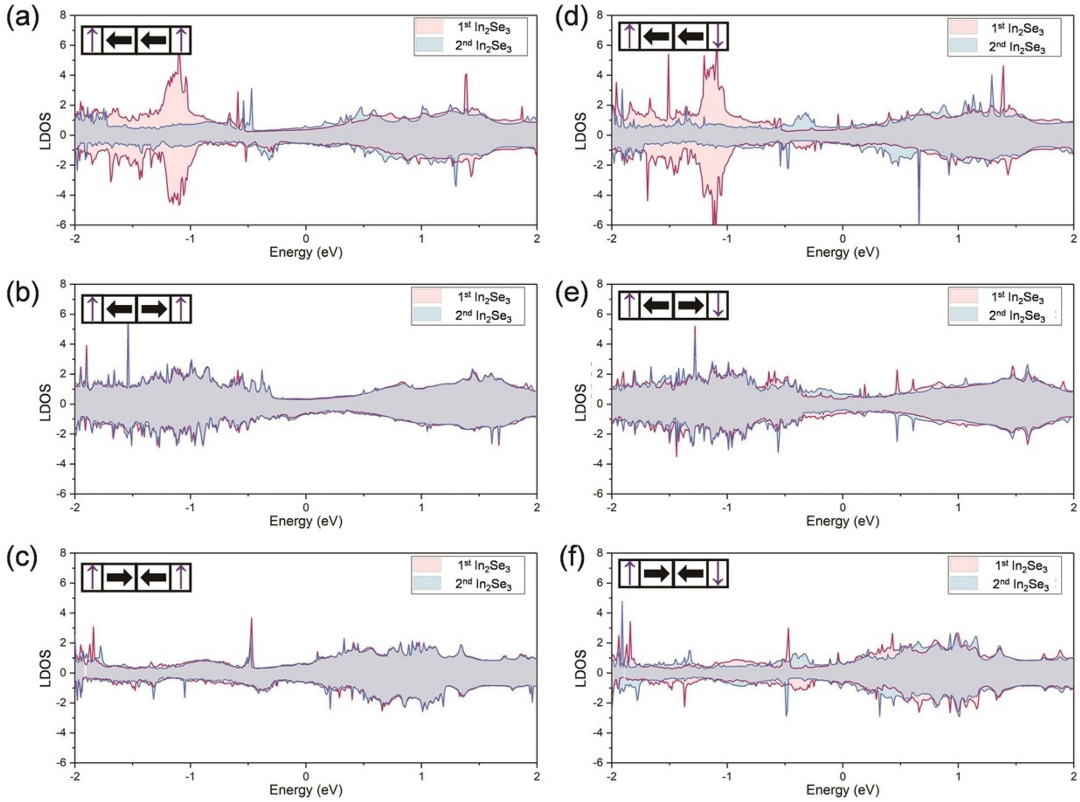

Fig. S5 Local density of state (LDOS) of NIN for (a)-(c) parallel magnetization and (d)-(f) antiparallel magnetization alignment. (a) and (d) are $P_{\leftarrow\leftarrow}$ barrier. (b) and (e) are $P_{\leftarrow\rightarrow}$ barrier. (c) and (f) are $P_{\rightarrow\leftarrow}$ barrier.

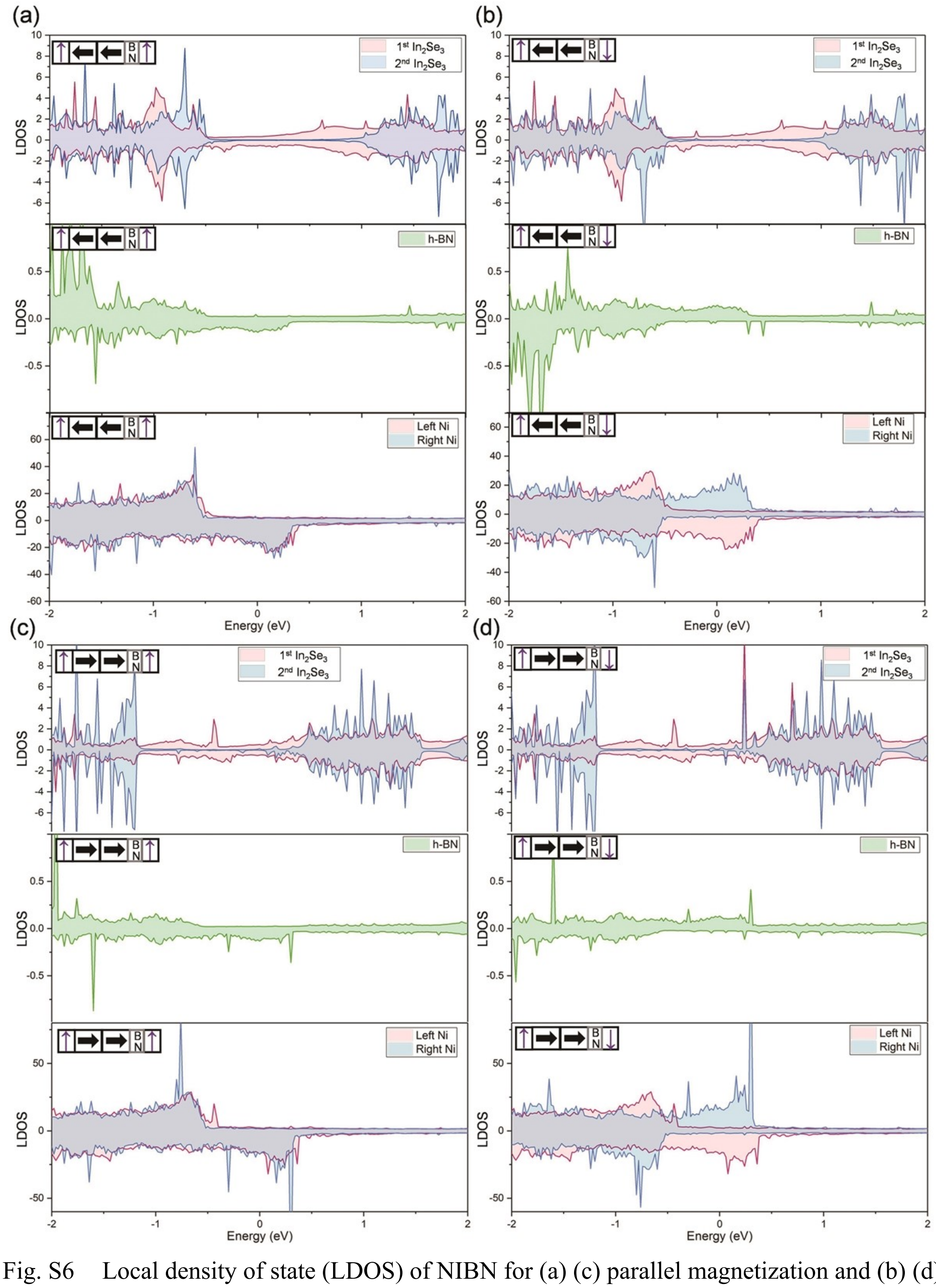

Fig. S6 Local density of state (LDOS) of NIBN for (a) (c) parallel magnetization and (b) (d) antiparallel magnetization alignment. (a) and (b) are $P_{\leftarrow\leftarrow}$ barrier. (c) and (d) are $P_{\rightarrow\rightarrow}$ barrier.

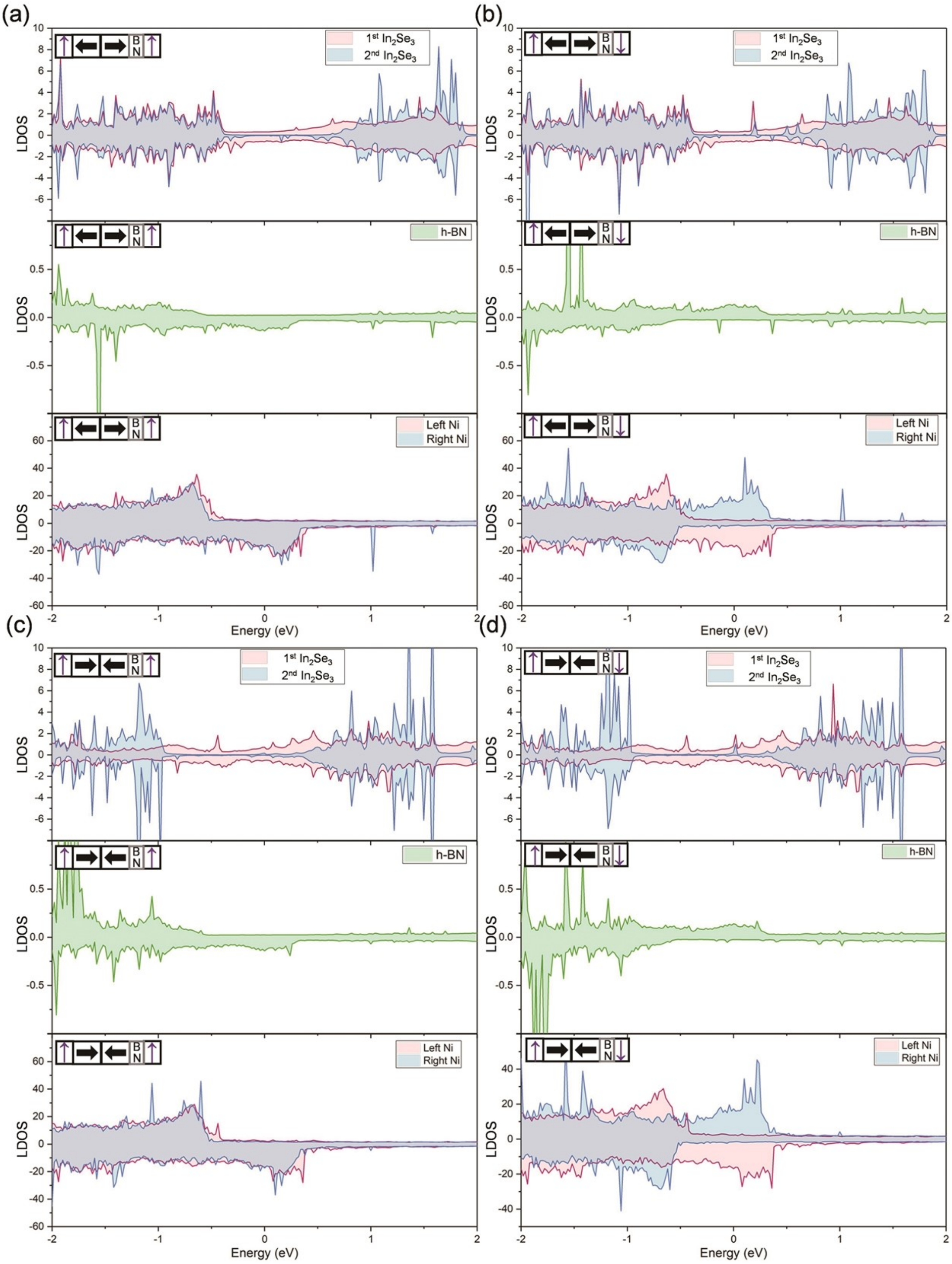

Fig. S7 Local density of state (LDOS) of NIBN for (a) (c) parallel magnetization and (b) (d) antiparallel magnetization alignment. (a) and (b) are $P_{\leftarrow\rightarrow}$ barrier. (c) and (d) are $P_{\rightarrow\leftarrow}$ barrier.

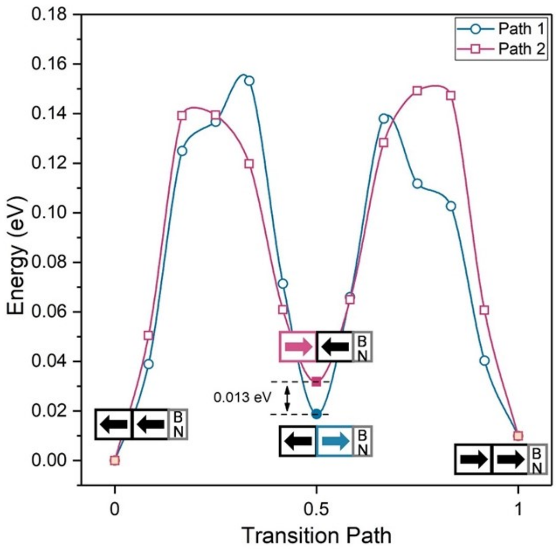

Fig. S8 The transition path for 2L-In_2Se_3/h-BN heterostructure.

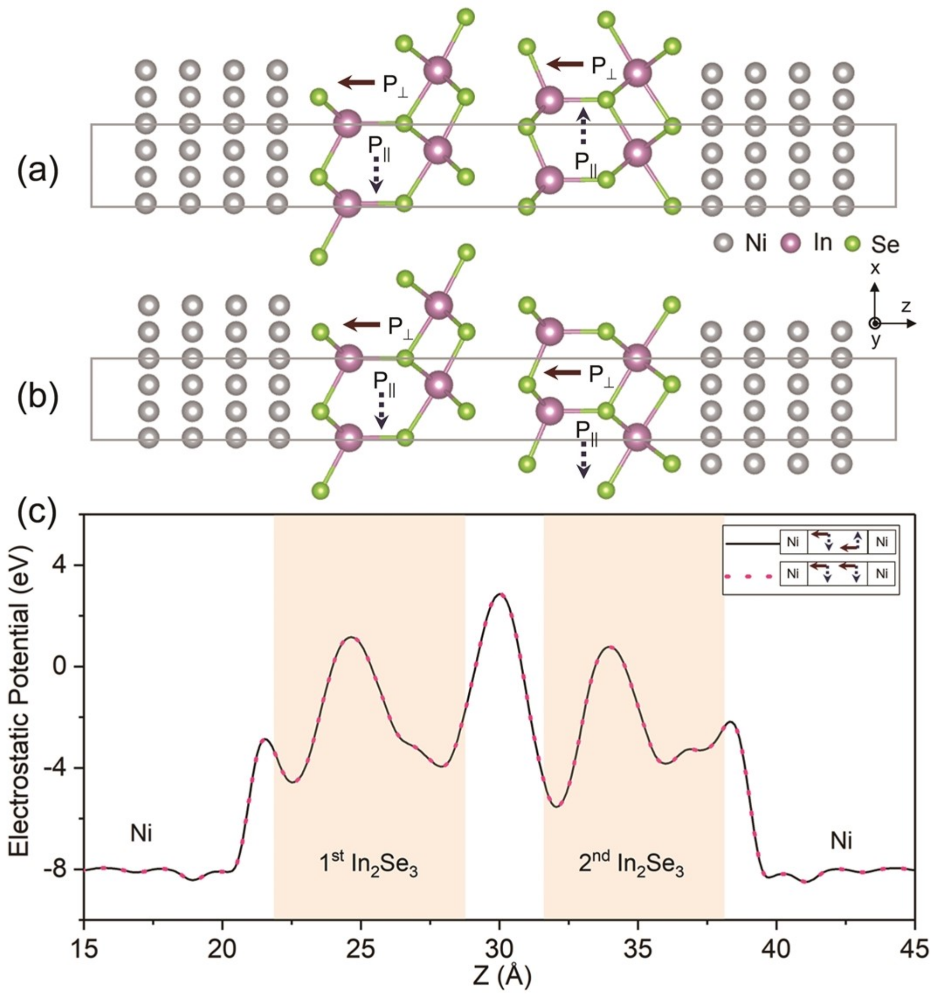

Fig. S9 Atomic structures of Ni/2L-In_2Se_3/Ni (NIN) with In_2Se_3 in (a) 2H stacking and (b) 3R stacking. (c) The in-plane averaged electrostatic potentials of NIN tunnel junction along the out-of-plane direction.

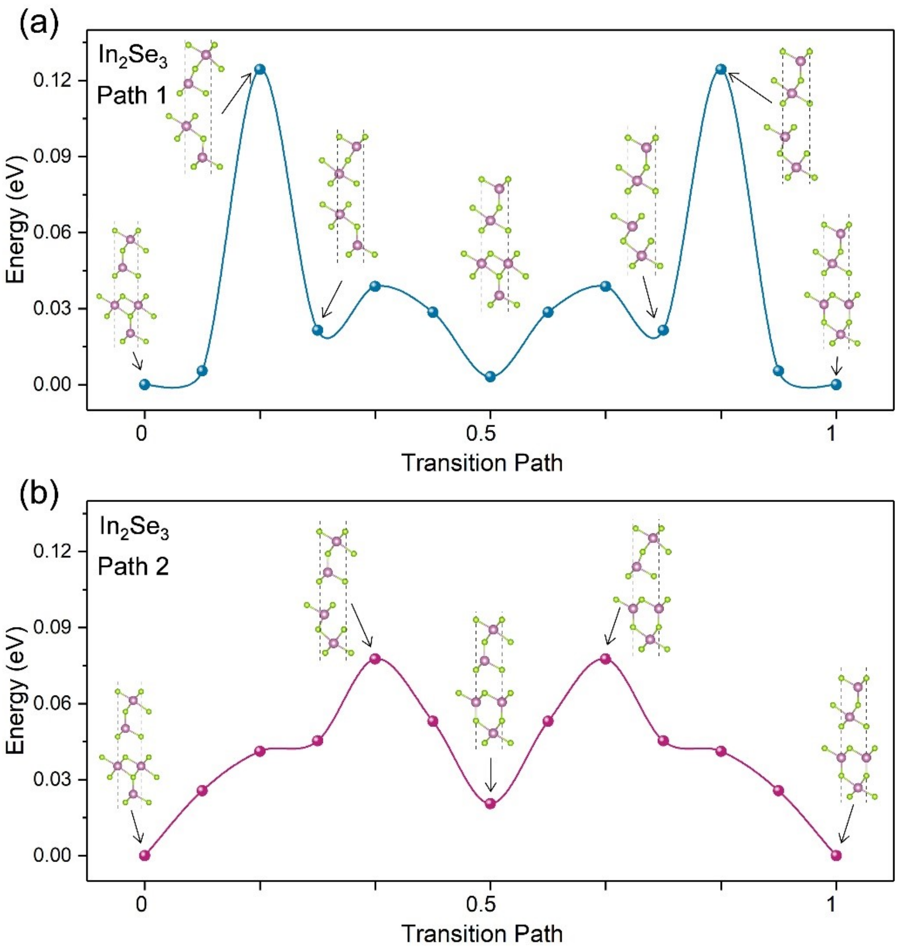

Fig. S10 Total energy along the transition path with the atomic structures of 2L-In_2Se_3 corresponding to the local maximum and local minimum points. (a) Path 1 with tail-to-tail ($P_{\leftarrow\rightarrow}$) metastable antiferroelectric state. (b) Path 2 with head-to-head ($P_{\rightarrow\leftarrow}$) metastable antiferroelectric state.

TABLE S1. Transmission coefficients of NIN and NIBN tunnel junctions in different Ni magnetic polarization states.

		$M_{\uparrow\uparrow}$			$M_{\uparrow\downarrow}$		
		$T_{\uparrow}$(spin up)	$T_{\downarrow}$(spin down)	T_{total}	$T_{\uparrow}$(spin up)	$T_{\downarrow}$(spin down)	T_{total}
NIN	$P_{\leftarrow\leftarrow}$	0.0141	0.0216	0.0357	0.0091	0.0157	0.0248
	$P_{\leftarrow\rightarrow}$	0.0188	0.0473	0.0661	0.0187	0.0202	0.0389
	$P_{\rightarrow\leftarrow}$	0.0701	0.0329	0.103	0.0347	0.0724	0.056
NIBN	$P_{\leftarrow\leftarrow}$	0.0000747	0.000609	0.000684	0.000106	0.0000640	0.000170
	$P_{\leftarrow\rightarrow}$	0.0000797	0.00110	0.00118	0.000105	0.0000829	0.000188
	$P_{\rightarrow\leftarrow}$	0.00136	0.00397	0.00533	0.00214	0.000114	0.00225
	$P_{\rightarrow\rightarrow}$	0.000981	0.00631	0.00729	0.000903	0.000167	0.00107

Reference

1. M. Brandbyge, J. L. Mozos, P. Ordejon, J. Taylor and K. Stokbro, *Phys. Rev. B*, 2002, **65**,

165401.